Chapter - 4

Simple uniaxial pressure device for ac-susceptibility measurements suitable for closed cycle refrigerator system

4.1 Introduction

Recent studies on strongly correlated systems have uncovered a wealth of fascinating physics that has challenged our fundamental understanding and cannot be understood by conventional existing theories. Many strongly correlated electrons systems such as high T_c superconductors, ruthenates, cobaltates, and manganites are characterized by a strong interplay of charge, spin, and orbital order because of which the lattice exhibit exotic physical phenomena [1-4]. The investigation of magnetic properties at high pressure and low temperature is undoubtedly one of the important tasks for the basic understanding of various critical magnetic phenomena in superconductors and manganites [1-6]. Recent studies on various strongly correlated systems suggested that variations of the lattice by pressure play a crucial role in varying transport, magnetic and structural properties [6-13]. Hence, in strongly correlated systems uniaxial pressure experimental technique is considered to be an important tool in playing with spin, orbital, and charge order at low temperature [6, 14 -17].

Ac-susceptibility is an important experimental tool for investigating electronic and magnetic properties of superconductors, manganites, and other strongly correlated systems. Further, ac-susceptibility measurements avoid the burden of attaching leads to the sample, which is really a difficult task in the case of small size single crystals. Transport and magnetic measurements under uniaxial pressure with different techniques were used for different

purposes [16-23]. There are several reports on the measurement of dc magnetization under direct uniaxial pressure using commercial superconducting quantum interference device (SQUID) magnetometer [16-18], ac-susceptibility technique using strain gauge as the pressure sensor at low temperatures [20-21], resistivity using clamp-type technique [24] and continuous direct uniaxial pressure using disc-micrometer and spring holder attachment with closed cycle refrigerator system (CCRS) [25].

There are many reports of instrumentation in literature on ac-susceptibility measurements with modification in the Hartshorn mutual inductance bridge and compensation circuits at ambient pressure down to 1.5 K [27-31]. There are only few reports of instrumentation on direct uniaxial pressure techniques for doing ac-susceptibility measurements using continuous flow helium gas [19, 26]. In literature there is no report on the measurement of ac-susceptibility under direct uniaxial pressure using CCRS. Hence, the present work is to design a simple ac-susceptibility measurement setup under uniaxial pressure down to 30 K using CCRS.

4.2 Details of the experimental setup

The experimental setup consists of uniaxial pressure device, uniaxial pressure cell, coil system, temperature measurement and control, automation, and closed cycle refrigerator system. The details of uniaxial pressure device for the measurement of electrical resistivity are given in earlier report [25]. The important aspects of the present setups are described in the following sections.

4.2.1 Uniaxial pressure cell

A new miniature uniaxial pressure cell has been developed for ac- susceptibility measurements, which is suitable for CCRS. The mechanical diagram of the miniature uniaxial pressure cell with inclusion of bobbin and the coils and with the corresponding dimensions in the millimeter scale is shown in Fig 4.1. The pressure cell is made of nonmagnetic high purity Be (2%)-Cu alloy with 20 mm diameter, which is suitable for ac-susceptibility measurements under pressure. The pressure cell has a bore of 11 mm diameter and 37 mm depth for accommodating the bobbin and the coils, and this inner space of the bobbin is enough for assembling the sample and the passage for transmitting rod. The anvils are made of Be (2%)-Cu alloy of 5 mm diameter. The sample (oriented crystal to be investigated) is kept at the centre of one of the secondary coils, which is close to the bottom of the uniaxial pressure cell.

Inorder to have easy mounting and demounting of the anvils and coils into the pressure cell two slots are provided on both sides with 2.5 mm width and 22 mm length from the top of the pressure cell. A hole of 1.5mmϕ is provided at the bottom of the pressure cell. To facilitate easy mounting of pressure cell on the cold head of the CCRS, the male and female threads are made at the bottom of the pressure cell and the top of the cold head of the CCRS, respectively. In order to achieve better thermal contact Apieson grease is used in between the bottom of the pressure cell and the top of the cold head of the CCRS. The bottom of the top anvil and top of the bottom anvils are coated with a thin layer of GE varnish, and the sample is kept on the bottom anvil with GE varnish.

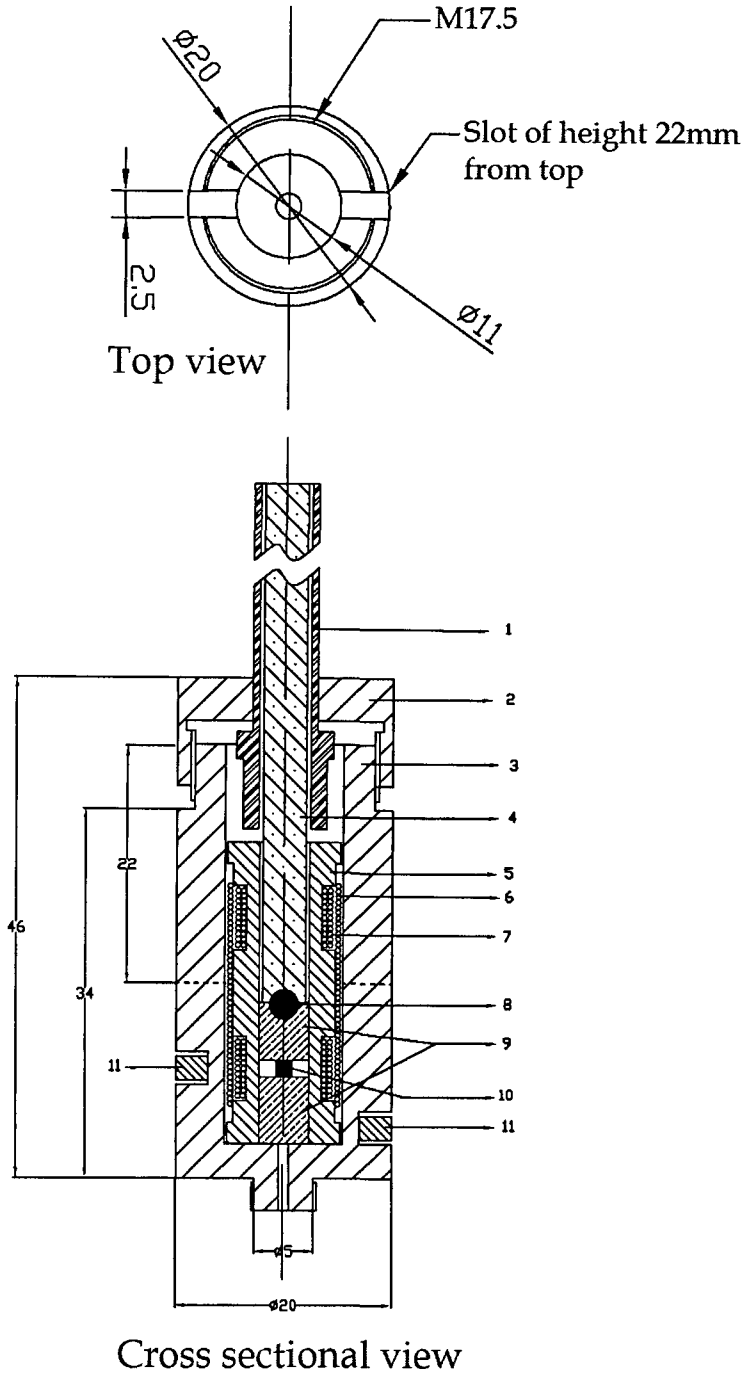

Figure 4.1 Mechanical diagram of the miniature uniaxial pressure cell with ac-susceptibility coils.
[1. SS pressure transmitting rod guiding tube, 2. Locking nut, 3. Be-Cu alloy, 4. SS pressure transmitting rod, 5. Teflon bobbin, 6. Primary coil, 7. Secondary coil, 8. SS ball, 9. Be-Cu anvils, 10. Sample, and 11. Cernox temperature sensor.]

4.2.2 Coil system

The present ac-susceptibility measurement is based on the mutual inductance technique. The primary and secondary coils have been wound in the same bobbin made of stycast #1266 or Delrin, and the detailed mechanical diagram and the photograph are shown in Figs. 4.2 (a) and 4.2 (b) respectively. The stycast #1266 is chosen because its high thermal conductivity and low diamagnetic susceptibility and because it is easy to machine. It also has low thermal expansion coefficient, which ensures a constant ac field inside the primary coil at all temperatures. The two secondary coils are wound directly on a Delrin bobbin with equal number of turns but in opposite directions, using a single insulated copper wire (SWG 45) without any soldering joints. These secondary coils are positioned on the same axis and connected in series. A gap of 7 mm is provided between two secondary coils to obtain a better signal and to reduce the field overlaps of the two coils. The secondary coils are covered by a thin layer of GE varnish on which the primary coil is wound. The primary coil is placed over the secondary coils in order to get more signals from the sample under uniaxial pressure. The offset in the induced voltage due to incomplete compensation has to be reduced to the least possible level. This is done to increase the sensitivity of the coils. Adding or taking away of the turns of the secondary coil caries out the compensation at room temperature. Coating of GE varnish minimizes the noise over secondary and primary coils. An offset voltage of less than 2 microvolt has been obtained in the present measurement.

The specifications of coils are listed in Table I. The primary and secondary coil leads are taken out from the two slots provided on either sides of the pressure cell. The destruction of coil under pressure is remote and so the same coil can be used for several measurements.

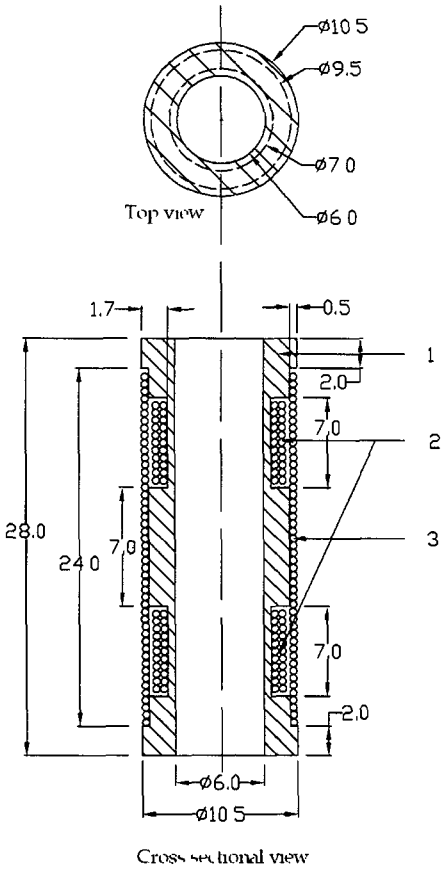

Figure 4.2 (a) Mechanical diagram of the bobbin with coil
[1. Delrin bobbin, 2. Secondary coils, and 3. Primary coil]

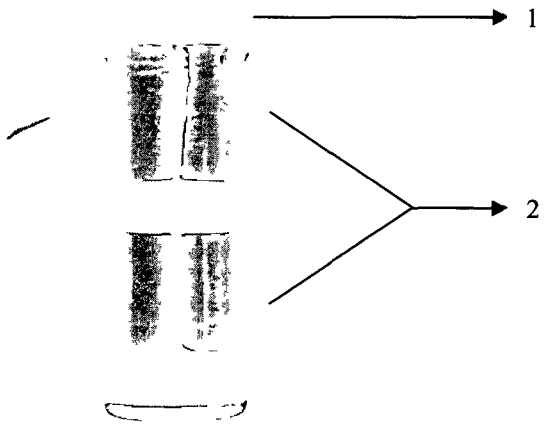

Figure 4.2 (b) Photograph of the bobbin with coil (Primary coil not shown)
[1. Delrin bobbin, 2. Secondary coils]

Table I. Coil specification:

Dimension of copper wire	SWG 45
Length of primary coil	24 mm
Length of secondary coils	7 mm
Number of turns in primary coil	400
Number of turns in secondary s coils	600 and 600+Δ
Distance between the centre of secondary coils	14mm
Inductance of primary	0.51 mH
Inductance of secondary coils	4.35 mH
Room temperature resistance of primary coil	65Ω
Room temperature resistance of Secondary coils	150Ω

4.3 Temperature measurement, control and automation

The schematic diagram of uniaxial pressure device mounted on CCRS is shown in Fig. 4.3. In the temperature measurement two calibrated Cernox sensors (CX1050) are used. One is attached at the bottom of the pressure cell to measure the temperature of the sample, and another is attached to cold head of the CCRS, to control the temperature through Lakeshore low temperature controller (331). The data is collected using LABVIEW software and general purpose interface bus (GPIB) card. The block diagram of the automated data collection is shown in Fig. 4.4. A low noise and high stable signal compensatory circuit is used to measure absolute value of ac susceptibility as reported by Slade *et al* [32]. The measurement of the absolute susceptibility under uniaxial pressures for manganites and superconductors is not required, and hence a compensatory circuit was not used.

4.4 Measurement procedure and calibration

The primary coil is energized by a constant current with a frequency of 810 Hz from the internal oscillator of digital signal processing (DSP) Lock-in amplifier (SR850) for susceptibility measurements. The output from the secondary is detected by the same Lock-in amplifier. Ac-susceptibility in the empty coil at atmospheric pressure down to 30 K was measured in order to confirm that there is no appreciable change in the signal due to Delrin or stycast #1266 in the present setup.

The measurement of ac-susceptibility is calibrated in the temperature range of 30-300 K at atmospheric pressure using high purity standard paramagnetic salts [Gd_2O_3, Er_2O_3, $Fe(NH_4SO_4)_26H_2O$], Fe_3O_4, Gd metal, and Dy metal. The relationship between the inverse susceptibility and temperature of Gd_2O_3, and Er_2O_3 are shown in Fig. 4.5. The susceptibility as a function of weight of Fe_3O_4 and $Fe(NH_4SO_4)_26H_2O$ samples at atmospheric pressure is shown in Fig. 4.6.

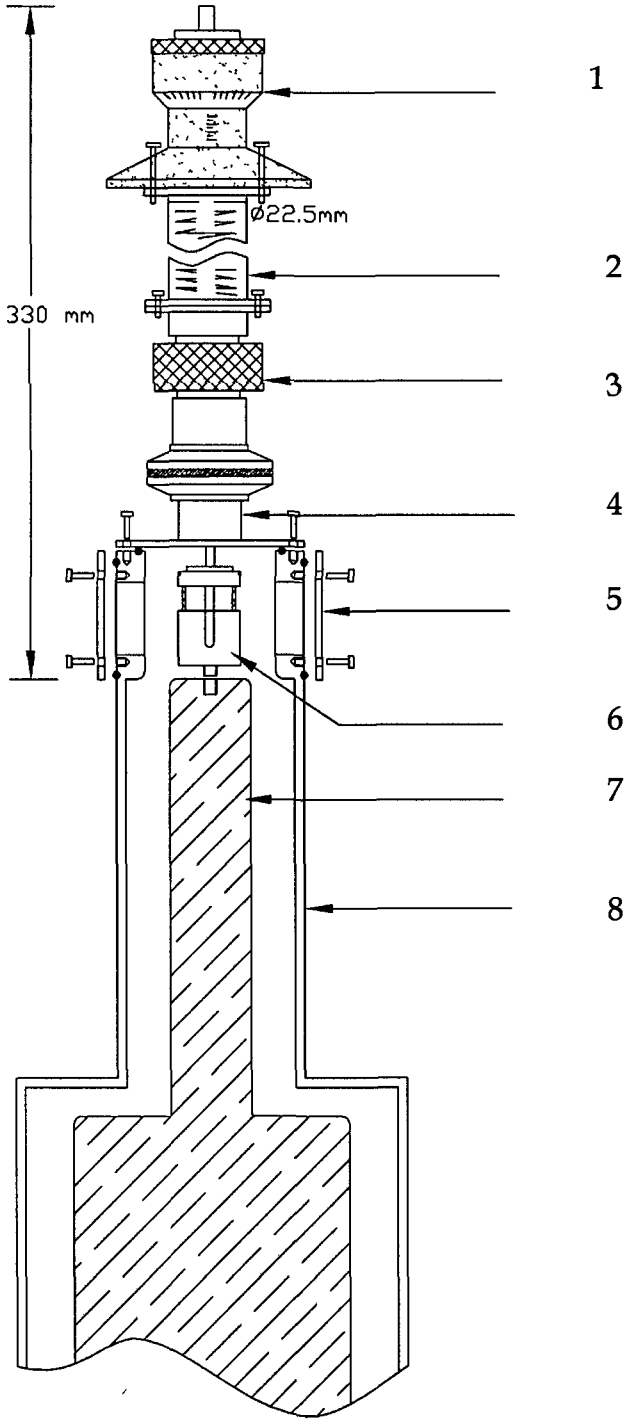

Figure 4.2 (a) shows the mechanical diagram of the uniaxial pressure device with indication of main parts of the device and the corresponding dimensions.

[1. Disc micrometer, 2. SS spring, 3. Wilson seal, 4. Demountable top-dummy plate, 5. Side window for access, 6. Uniaxial pressure device, 7. CCR Cold head, 8. Vacuum shroud]

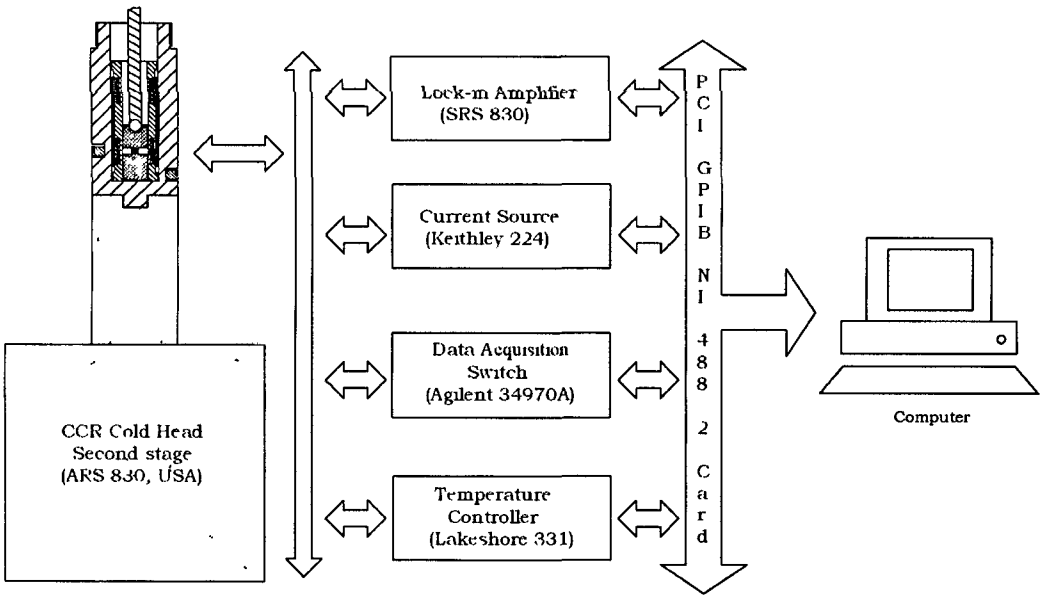

Figure 4.4 The block diagram of the experimental setup used for automated data collection

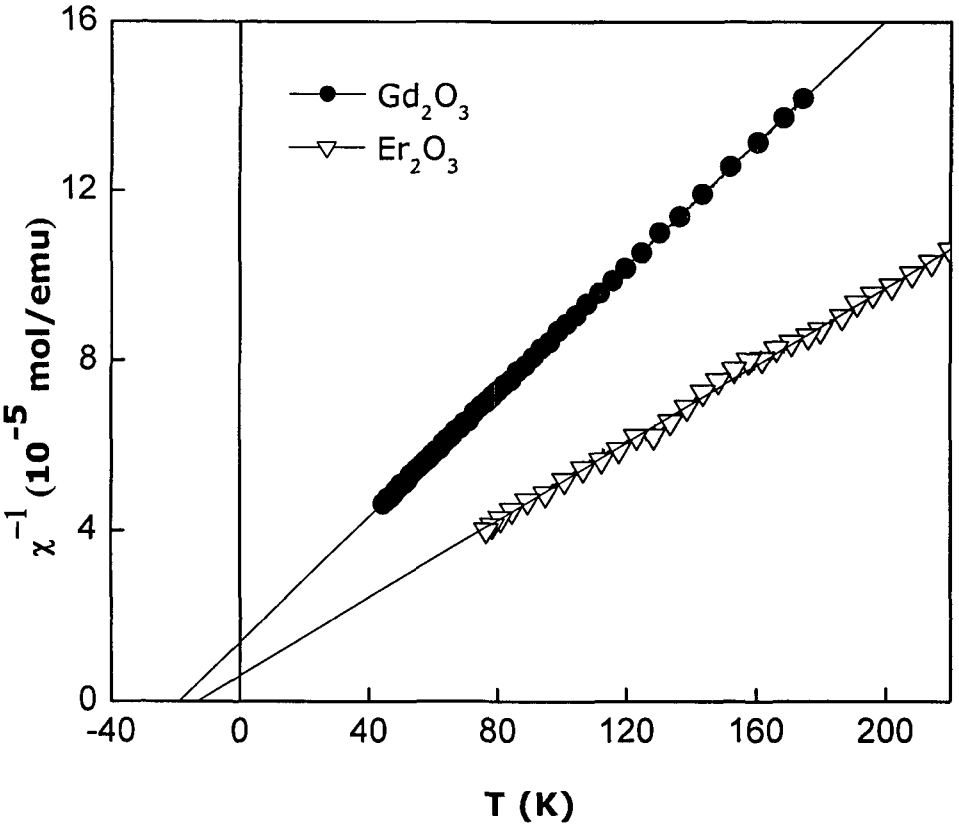

Figure 4.5 Curie - Weiss plot for Gd_2O_3, and Er_2O_3

The inverse susceptibility vs. temperature of $Fe(NH_4SO_4)_26H_2O$ material is shown as an inset in Fig. 4.6. The values of Curie constant are obtained from the slope of the experimental data and compared with data in the literature [28, 33-35], and are in good agreement as shown in Table II. Furthermore, the frequency dependences of the ac-susceptibility of standard paramagnetic salts at room temperature at atmospheric pressure

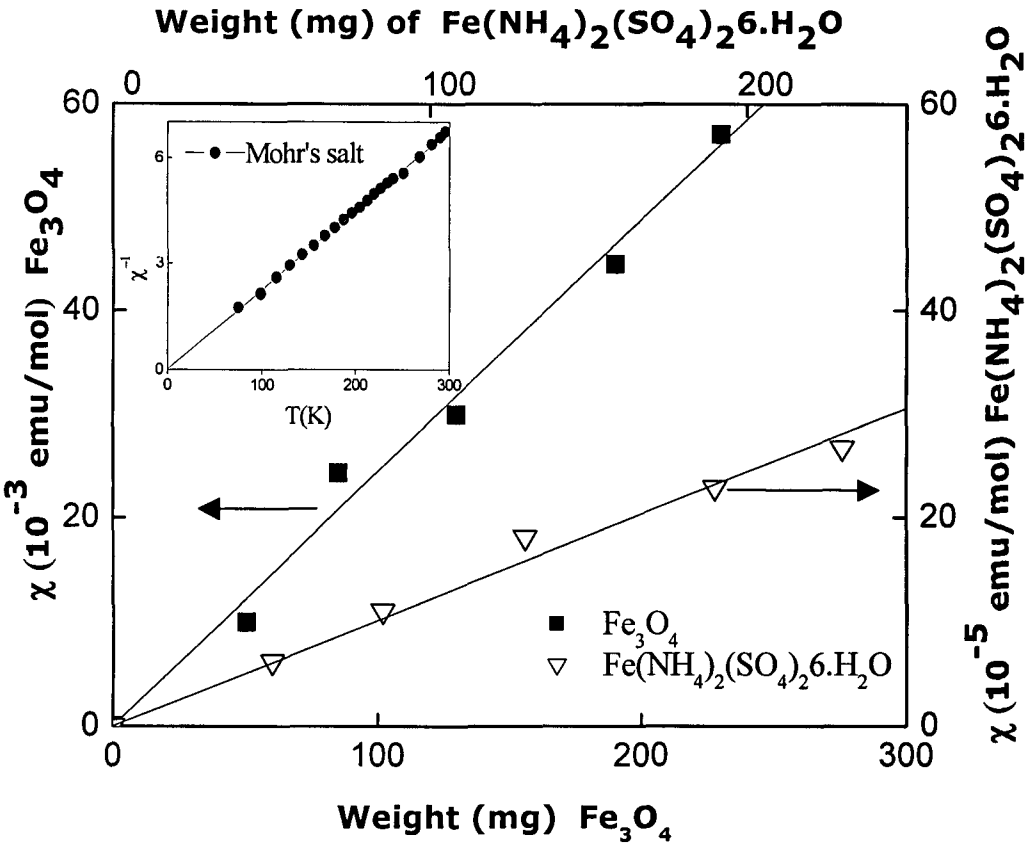

Figure 4.6 A plot of ac-susceptibility (χ) as a function of weight [Fe_3O_4 and $Fe(NH_4SO_4)_26H_2O$] samples at atmospheric pressure. (Insert: χ^{-1} vs T ($Fe(NH_4SO_4)_26H_2O$)

Table II. The values of Curie constant and other experimental parameters of standard samples of our experimental data are compared with literature

	C (cm^3 K mol^{-1})		θ (K)	
Sample	Fitted	Literature	Fitted	Literature
Gd_2O_3	8.6±0.01	8.3	-18.03±2	-18.4
Er_2O_3	.....	11.1	-12.40±1	-13.4

were measured to identify the region of frequency in which the output from the secondary is linear in the present setup. The frequency of 810 Hz was chosen for all susceptibility measurements.

4.5 Performance of the system

The ac-susceptibility as a function of temperature on various magnetic materials were measured to show various kinds of transitions such as the superconducting transition of yttrium barium copper oxide (YBCO) [19], ferromagnetic transitions of Gd metal and Dy metal [34-35], spin glass transition of $Pr_{0.8}Sr_{0.2}MnO_3$ (PSMO) [36], and metal-insulator transition of $La_{0.85}Ba_{0.15}MnO_3$ (LBMO)[37]. The temperature dependence of the ac-susceptibility of Gd and Dy metals are shown in Fig. 4.7.

The temperature dependence of the ac-susceptibility of YBCO and PSMO systems and the corresponding transition temperatures agreed very well with the literature and are shown in Fig. 4.8. These measurements are taken to prove the capability of the present design of the ac-susceptibility measurements at atmospheric pressure to detect the various transitions without using any external compensatory electronic circuits. The performance of the uniaxial pressure device is demonstrated by investigating the uniaxial pressure dependence of LBMO single crystal. The ac-susceptibility as a function of temperature for LBMO at various uniaxial pressures (P$||$c-axis) upto 46 MPa is shown in Fig. 4.9 and it is found that the Curie temperature (T_c) decreases ($dT_c/dP_{||c\,axis} = -11.65$ K/GPa) with the increase of pressure.

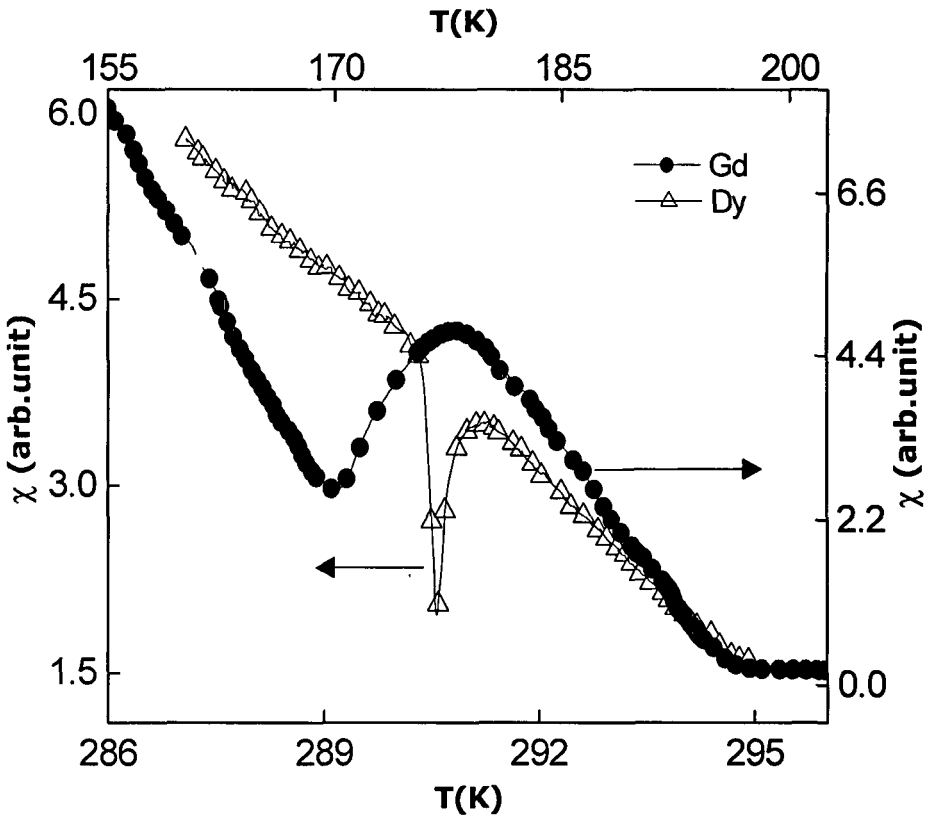

Figure 4.7 Temperature dependence of ac-susceptibility (χ) of dysprosium and gadolinium, metals in the region of Curie temperature

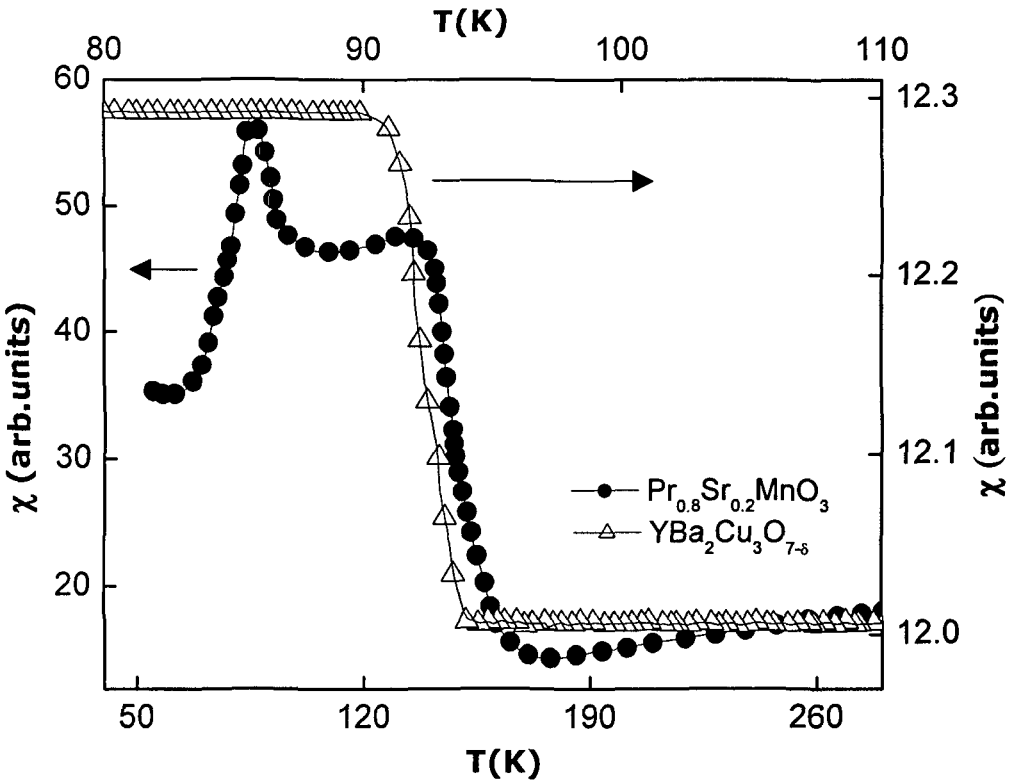

Figure 4.8 Variation of ac-susceptibility (χ) as a function of temperature of superconductor $YBa_2Cu_3O_7$ and $Pr_{0.8}Sr_{0.2}MnO_3$ systems

4.6 Features

The design is simple, is user friendly, and does not require pressure calibration, and the calculation of pressure and changing of sample are easy and inexpensive. Measurement can even be made on thin and small size oriented crystals. The failure of the coil is remote under uniaxial pressure. The present setup can be used as a multipurpose uniaxial pressure device for the measurement of Hall effect and thermoelectric power with a small modification in the pressure cell.

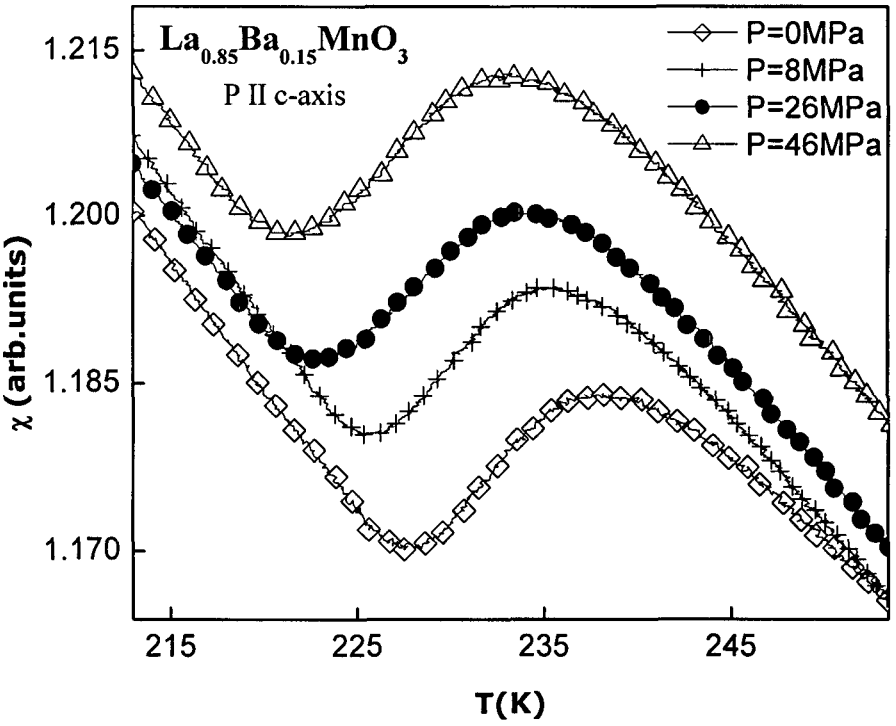

Figure 4.9 The ac-susceptibility as a function of temperature of LBMO for various uniaxial pressures (P | | c-axis) upto 46 MPa

References:

1. Y. Tokura, Colossal Magnetoresistive Oxides, (Gordon and Breach Science Publishers, London, 2000).
2. E. Dagotto, Nanoscale Phase separation and Colossal Magnetoresistance: The Physics of Manganites and Related Compounds, Springer Series in Solid State Sciences vol. 136 (Springer New York 2003)
3. P. Khalifah, K.D. Nelson, R. Jin, Z.Q. Mao, Y.Liu, Q.Huang, X.P.A.Gao, A.P. Ramirez, and R.J. Cava, Nature, **411**, 669 (2001)
4. J.M. Tranquada, B.J. Sternlib, J.D. Axe, Y. Nakamura, and S. Uchida, Nature, **375**, 561 (1995)
5. J.S.Zhou, and J.B. Goodenough, Phys. Rev. B, **56** 6288 (1997)
6. S. Arumugam, N.Mori, N. Takeshita, H. Takashima, T. Noda, H. Eisaki, and S.Uchida, Phys.Rev.Lett. **88**, 247001 (2002)
7. I.Fita, R. Szymczak, R.Puzniak, I.O. Troyanchuk, J. Fink-Finowicki, Ya.M. Mukovskii, V.N. Varyukhin, and H.Szymczak, Phys. Rev. B, **71**, 214404 (2005)
8. A.. Asamitsu, Y. Moritomo, Y. Tomoioka, T.Arima, and Y. Tokura, Nature, **373**, 407 (1995)
9. Y. Moritomo, A.Asamitsu, and Y. Tokura, Phys. Rev. B, **51**, 16491(1995)
10. P.G. Radaelli, D.E. Cox, M. Marezio, S.-W.Cheong, P.E. Schiffer, and A.P. Ramirez, Phys. Rev. Lett., **75**, 4488 (1995)
11. A.Gukasov, F.Wang, B. Anighoefer, L.He, R.Suryanarayanan, and A. Revcolevschi, Phys. Rev. B **72**, 092402 (2005).
12. M.Uehara, T.Nagata, J.Akimitsu, H. Takahashi, N. Mori, and K. Kinoshita, J. Phys. Soc. Japan, **65**, 2764 (1996).
13. R. Klingeler, J. Geck, S.Arumugam, N. Triston, P. Reutler, B. Buchner, L.Pinsard Gaudart, and A. Revcolevschi, Phys. Rev. B, **73**, 214432 (2006)
14. S.Arumugam, K.Mydeen, N.Manivannan, M.Kumaresa Vanji, D.Prabhakaran, A. T. Boothroyd, R.K.Sharma, and P. Mandal, Phys. Rev.B, **73**, 212412 (2006)

15. N. Zhang, W. Ding, Z. Guo, W. Zhong, D. Xing, and Y. Du, Phys. Lett. A, **219**, 319 (1996)
16. S. Ikeda, N. Shirakawa, T. Yanagiswa, Y. Yoshida, S.Koikegami, S.Koike, M. Kosaka, and Y.Uwatoko, J. Phys. Soc. Japan, **73**, 1322 (2004)
17. N. Takeshita, T. Sasagawa, T.Sugioka, Y. Tokura, and H. Takagi, J.Phys. Soc. Japan, **73**, 1123 (2004)
18. Y. Uwatoko, J.L. Sarrao, J.D. Thompson, N. Mori, and G. Oomi, Rev. High Pressure Sci. Technol., **7**, 479 (1998).
19. U. Welp, M. Grimditch, S. Fleshler, W. Nessler, J. Downey, G.W. Crabtree, and J. Guimpel, Phys. Rev. Lett. **69**, 2130 (1992)
20. C. Pfleiderer, E. Bedin, and B. Salce, Rev.Sci. Instrum **68**, 3120 (1997)
21. T. Yamamizu, M. Endo, M. Nakayama, N. Kimura, and H. Aoki, Phys.Rev. B, **69**, 014423 (2004).
22. G.Cao, L. Balicas, Y.Xin, J.E. Crow, and C.S. Nelson, Physica C, **387**, 245 (2003)
23. A.B. Beznosov, V.A. Desnenko, E.L. Fertman, C. Ritter and D.D. Khalyavin, Phys. Rev., B **68**, 054109 (2003)
24. T. Arima and K. Nakamura 1999, Phys. Rev. B **60** R15013 (1999).
25. S.Arumugam, K.Mydeen, M.Kumaresa Vanji, and N.Mori, Rev. Sci. Instrum.**76**, 083904 (2005)
26. H.A. Ludwig, R. Quenzel, S.I. Schlachter, F.W. Hornung, K. Grube, W.H. Fietz, and T. Wolf, J.Low Temp.Phys. **105**, 1385 (1996)
27. L. Hartshorn, J. Sci. Instrum. **2**, 145 (1925)
28. M. Prasad, R.R. Rao, and A.K. Ray Chaudhuri, J.Phys. E: Sci. Instrum. **19**, 1013 (1986)
29. A.F. Deutz, R.Hulstman, and F.J. Kranenburg, Rev.Sci. Instrum. **60**, 113 (1989)
30. A. Banerjee, A.K. Rastogi, M.Kumar, A. Das, A. Mitra, and A.K.Majumdar, J. Phy. E: Sci. Instrum., **22**, 230 (1989).
31. A. Bajpai, and A. Banerjee, Rev.Sci.Instrum. **68**, 4075 (1997)

32. S.B.Slade, G.Kassablan, and A.E. Berkowitz, Rev.Sci. Instrum. **67**, 2871 (1996)

33. C.M. Brodbeck, R.R. Bukrey, and J.T. Hoeksema, Rev.Sci. Instrum. **49**, 1279 (1978)
34. J.M.D Coey, V. Skumryev, and et. al., Nature **401**, 35 (1999)
35. R.V. Krishnan, and A. Banerjee, Rev. Sci. Instrum. **70**, 85 (1999)
36. N. Rama, V.Sankaranarayanan, and M.S.Ramachandra Rao, J. Appl. Phys., **99**, 08Q315 (2006)
37. P.Mandal , and B.Ghosh, Phys. Rev.B **68**, 014422 (2003)